Available online at www.sciencedirect.com

ScienceDirect

Energy Procedia 124 (2017) 604–611

Energy Procedia

www.elsevier.com/locate/procedia

7th International Conference on Silicon Photovoltaics, SiliconPV 2017

Silicon solar cells with heterojunction emitters and laser processed base contacts

Chen Jin[a,*], Isidro Martín[a], Gema López[a], Samuel Harrison[b], Gerard Masmitja[a], Pablo R. Ortega[a], Ramon Alcubilla[a]

[a] *Departament d'Enginyeria Electrònica, Universitat Politècnica de Catalunya, C/Jordi Girona 1-3, Mòdul C4, 08034 Barcelona, Spain*
[b] *INES-CEA, 50 Avenue du Lac Léman, BP 332, 73370 Le Bourget du Lac, France.*

Abstract

In this work, we report on a novel structure of Interdigitated Back-Contacted (IBC) solar cells on c-Si p-type substrates that combines laser processed homojunction base contacts and silicon heterojunction (SHJ) emitters. These hybrid devices which can lead to potential benefits in device processing and/or conversion efficiency. In the proposed fabrication process special attention has been paid to the compatibility of both involved technologies: silicon heterojunction and laser doping from dielectric films. In particular, we focus on the surface passivation obtained by the heterojunction emitter after removing the aluminum oxide/silicon carbide (Al_2O_3/SiC_x) layer stack needed for the laser doping process and previously deposited on the c-Si surface. A severe passivation degradation after plasma etching process to remove the top SiC_x film is observed, despite leaving the Al_2O_3 film on the c-Si surface. Based on high-frequency capacitance-voltage characterization, an increase in the interface state density and a strong impact on the fixed charge density is deduced. Next, in order to choose an optimized metallization technology that could simultaneously contact both the ITO film and the p^+ laser processed regions, we evaluate the contact quality of Titanium and Aluminum on ITO. Results show that Titanium is a better option with a specific contact resistance of 1.1 mΩ·cm^2. Finally, finished hybrid IBC solar cells with conversion efficiencies in the 18-19% range are reported.

© 2017 The Authors. Published by Elsevier Ltd.
Peer review by the scientific conference committee of SiliconPV 2017 under responsibility of PSE AG.

Keywords: DopLa cell, heterojunction, laser doping, back-junction, c-Si solar cells.

* Corresponding author. Tel.: +34-93-4054193; fax: +34-93-4016756.
E-mail address: chen.jin@upc.edu

1876-6102 © 2017 The Authors. Published by Elsevier Ltd.
Peer review by the scientific conference committee of SiliconPV 2017 under responsibility of PSE AG.
10.1016/j.egypro.2017.09.084

1. Introduction

In the last years, our research group has been developing a novel structure of crystalline silicon (c-Si) solar cell called DopLa (Doped by Laser) cell where all the highly-doped regions are created by laser processing dielectric films [1-4]. The n^+ regions are formed by processing a phosphorus-doped silicon carbide film stack (SiC_x(n)) while the p^+ regions are based on aluminum oxide/silicon carbide (Al_2O_3/SiC_x) film. Apart from working as dopant sources, these films provide c-Si surface passivation and anti-reflection properties. This technology has been applied to Interdigitated Back-Contacted solar cells leading to DopLa-IBC devices [1].

In reference [1], a conversion efficiency of 15.5 % is reported for DopLa-IBC solar cells with V_{oc} = 644 mV, J_{sc}= 37.2 mA/cm^2 and *FF*= 65.1 %. The main limitations for those devices were the low V_{oc} and *FF* values attributed to high recombination at the laser processed emitter regions and the distance between them. A low temperature alternative to create the emitter regions is silicon heterojunction (SHJ). This technology is based on the formation of selective contacts through the deposition of an intrinsic and doped amorphous silicon films and it has been previously applied to IBC solar cells with excellent results [5-7]. In this work, we report on p-type IBC solar cells where we combine a SHJ emitter together with laser processing to create the base contacts. In particular, the emitter consists of thin intrinsic and phosphorus-doped amorphous silicon films (i/n a-Si:H) contacted by ITO, while for the base contacts, p^+ regions created by laser processed Al_2O_3/SiC_x films are defined. With this hybrid devices, we would like to overcome the V_{oc} and *FF* limitations observed for DopLa-IBC and explore the possible benefits of the combination of both low temperature technologies.

2. Experimental

The solar cell processing is based on a 280 µm-thick 2.5 Ω·cm FZ c-Si wafer with random pyramids textured front surface and polished rear surface. After a standard RCA cleaning, a 50 nm-thick Al_2O_3 film is symmetrically deposited on both surfaces by Atomic Layer Deposition technique, followed by a 10 minutes annealing at 400 ºC to activate the Si surface passivation. Then, the front Al_2O_3 film is capped by a 35 nm-thick SiC_x layer by PECVD in order to reduce optical reflection and protect the Al_2O_3 film from subsequent wet chemical steps. On the rear surface, we deposit a 50 nm-thick SiC_x layer in order to protect Al_2O_3 film and improve the laser process to create the p^+ regions [3]. After a photolithographic step on the rear surface, emitter windows are opened through SiC_x layer by CF_4/O_2 plasma etching. Next, the sample is treated by RCA1 cleaning and HF (1%) dip to remove the Al_2O_3 film at the emitter regions and expose the c-Si surface. Immediately after the cleaning, an intrinsic a-Si:H (~4 nm) and phosphorus-doped a-Si:H (~15 nm) film are deposited continuously onto the rear surface by PECVD at 300 ºC creating the silicon heterojunction at the opened emitter windows which is contacted by a 100 nm ITO layer deposited by RF sputtering. A second photolithographic step is used to remove ITO and i/n a-Si:H films by HF (2%) solution and HF/HNO_3 mixture solution respectively from the regions where the base contacts are to be defined.

Now, p^+ highly-doped regions are created by laser processing Al_2O_3/SiC_x stacks with a Q-switched Nd:YAG laser (StarMark SMP 100II Rofin-Baasel) emitting at 1064 nm in TEM00 with a power of 1.07 W, which is the minimal power for effective laser doping in order to avoid any possible damage on adjacent heterojunction [1]. The distance between each laser spot is 250 µm as developed in previous work [1]. Finally, the sample is metallized just after the laser step by Ti(~20 nm)/Al(~4µm) stack deposited by sputtering. In order to separate emitter and base contacts, a 50 µm gap of metal is defined by photolithography and subsequent Al etching with orthophosphoric acid/isopropanol mixture solution at 65 ºC followed by Ti etching with 1% HF solution. A detailed fabrication process of these hybrid devices on p-type substrate are summarized in the Table 1, while the resulting device structure is sketched in Figure 1.(a) and a microscope picture of the finger structure on rear surface is shown in Figure 1.(b).

Table. 1. Fabrication process of hybrid devices on p-type substrate.

Standard RCA cleaning
50 nm Al_2O_3 ALD deposition
SiC_x PECVD deposition on front surface (35 nm ARC coating) and rear surface (50 nm)
Emitter windows lithography and plasma etching
RCA1 and HF (1%) dip
Intrinsic and n-type a-Si:H PECVD deposition
ITO sputtering deposition
Base region lithography and ITO/a-Si:H wet etching
Base laser doping process
Sputtering 20 nm Ti and 4 µm Al deposition
Interdigitated contact definition

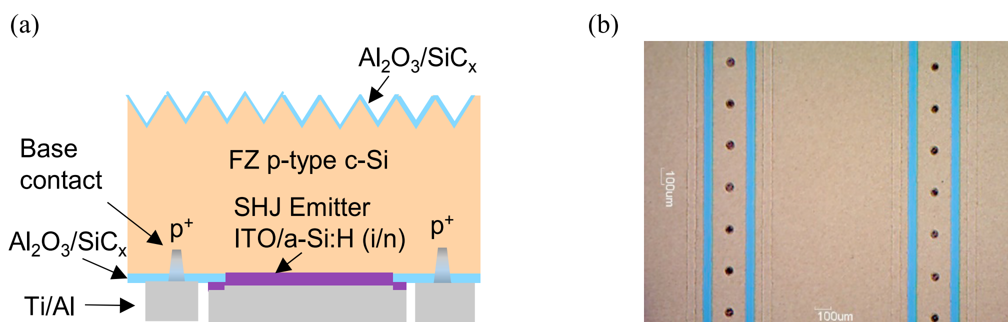

Fig. 1. (a) Cell structure of the fabricated p-type hybrid devices; (b) Microscope picture of the finger structure.

3. Results and discussion

3.1 Surface passivation measurements

As it can be seen in the fabrication process shown in Table 1, a crucial point of the combination of SHJ and laser doping technology is the passivation quality of the a-Si:H films after the etching the Al_2O_3 film previously deposited onto c-Si surface. To check out this passivation, we fabricated test samples reproducing the conditions that would be found in the final devices. In Figure 2.(a), we show the lifetime measurements of a sample symmetrically covered with 50 nm of Al_2O_3 deposited by ALD and 50 nm of stoichiometric SiC_x film deposited by PECVD. As it can be seen, lifetime is very close to the intrinsic lifetime (where only Auger and radiative recombination is considered [8]) indicating an excellent surface passivation quality. Then, SiC_x film is etched by plasma etching based on CF_4/O_2 mixture on one side leaving the Al_2O_3 film still fully covering the c-Si surface. Surprisingly, lifetime dramatically decreases below 10 µs indicating a poor surface passivation at the Al_2O_3/c-Si interface that has been exposed to the plasma. In the final solar cells, the highly recombining interface is only located at places where the Al_2O_3 will be chemically etched during the RCA1 cleaning prior to a-Si:H deposition. In the test sample, we performed the cleaning steps and the a-Si:H+ITO deposition. As it can be seen in figure 2.(a), lifetime is recovered to the initial passivation levels. This result indicates that the poor passivation is related to a modification of Al_2O_3/c-Si interface properties.

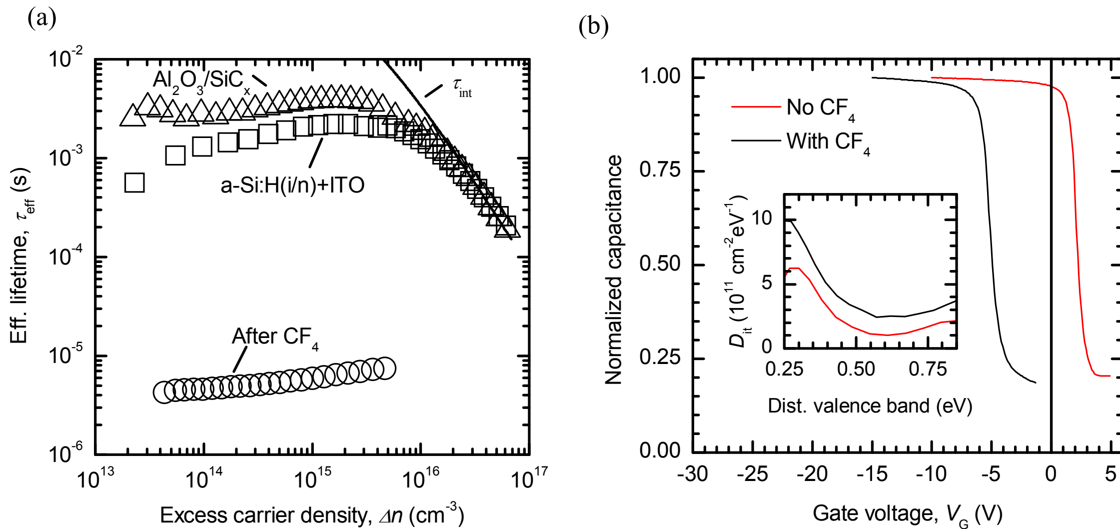

Fig. 2. (a) Lifetime measurements p-type hybrid device (b) Normalized capacitance voltage measures acquired at 1 MHz

In order to get a deeper knowledge of the impact of CF_4/O_2 plasma etching on passivation of Al_2O_3, we prepared Metal Insulator Semiconductor (MIS) capacitors consisting of Al/Al_2O_3/c-Si. For this experiment we used two type of samples. On the one hand, we deposit 50 nm thick Al_2O_3 film onto c-Si surface and a 400 ºC annealing for 10 minutes was carried out to increase the negative fixed charge density [9]. On the other hand, we deposit an Al_2O_3 (50 nm)/SiC_x (50 nm) stack where SiC_x was subsequently etched by CF_4/O_2 plasma etching. As a result, a similar 50 nm-thick Al_2O_3 film than in the previous case is left onto c-Si surface. A uniform aluminum layer is deposited onto rear surface of both samples by e-beam method followed by a full-area intensive point-laser firing forming ohmic contacts. Round-shape Aluminum dots with a nominal diameter of 2 mm are thermally evaporated onto the front surface using a shadow mask.

The measured high frequency (1 MHz) Capacitance-Voltage (*C-V*) curves for both samples are shown in figure 2.(b) where we have normalized the measured capacitance by the maximum capacitance measured under accumulation conditions. As it can be seen, the *C-V* curve is shifted to negative values after CF_4/O_2 plasma etching indicating the appearance of positive fixed charge (Q_f). Using conventional MIS theory [10], we could quantify Q_f for both samples from the shift of the flat band voltage and using a difference between metal and semiconductor workfunction of -0.628 eV. For the case without plasma etching, we obtain $Q_f = -1.9\times10^{12}$ cm^{-2} while after CF_4/O_2 plasma etching Q_f is positive and equal to 2.0×10^{12} cm^{-2}. This big difference indicates a strong impact of plasma etching on Al_2O_3 film configuration. Notice that the determined Q_f value is an equivalent charge located at the dielectric/c-Si interface, but the real charge distribution is not known. Probably, the positive charge is related to the first nanometers of the film that have been exposed to the plasma modifying surface configuration from accumulation to high inversion.

Additionally, we applied the method proposed by Terman [11] to calculate the interface state density (D_{it}) from the high-frequency *C-V* curve. In this method, D_{it} is obtained from the stretching out of the *C-V* curve along the voltage axis. It is more precise when surface is under depletion or low inversion conditions and capacitance is not constant. As a consequence, D_{it} is determined in an energy range around midgap which is the region of more interest from the recombination point of view. The obtained D_{it} values are plotted in the inset of figure 2.(b) where we can see that this parameter increases in all the explored energy range and more significantly close to the valence band when CF_4/O_2 plasma is applied. A quantitative justification of the dramatic lifetime decrease after plasma etching by the measured interface parameters is beyond the scope of this paper. However, we can conclude that *C-V* measurements reveal a strong impact of CF_4/O_2 plasma on Al_2O_3/c-Si interface.

3.2 Contact resistance on ITO

In previous experiments, p^+ laser doped regions were successfully contacted by Aluminum [4] and Titanium [1] while in our heterojunction solar cells ITO is typically contacted by Silver [12]. Since Silver is not a good option for p^+ doped c-Si, we decided to evaluate the contact quality of Aluminum and Titanium on ITO using the Transfer Line Method (TLM) [13]. In this method, metal contacts with different spacing between them are defined and the resistance between them is measured. Then, the total resistance (R_T) follows a linear trend depending on the distance between contacts (L) as follows:

$$R_T = \frac{R_S}{W} \times \left(L + 2L_T\right) \quad (1)$$

where W is the width of the contact and L_T is the transfer length indicating the average distance that a carrier travels in the silicon beneath the contact before it flows up into the contact. Consequently, the effective contact area can be regarded as $L_T \times W$. Finally, the specific contact resistance is calculated from the y-axis intercept applying a corrected contact area following equation (2):

$$\rho_C = R_C \times L_T \times W \quad (2)$$

We deposit Al and Ti by sputtering onto samples covered by same ITO through shadow mask that defines a series of rectangular-shape metal contacts with distinct spacing. In figure 3.(a), we show the *I-V* curves of ITO/Al and ITO/Ti contacts with the same spacing for ±1 V. It can be seen that Aluminum is creating a poorer contact on ITO even showing a rectifying trend for high voltages. On the contrary, ITO/Ti is perfectly linear with lower resistance. Based on these results, we performed TLM measurements only for the ITO/Ti contact. We reduced the explored voltage range to ±0.1 V in order to get a linear relation between current and voltage and R_T was measured from the inverse of the slope at V= 0.1 V for every contact spacing. The obtained values are shown in figure 3.(b) with the best linear fit. Applying equation (1) and (2), we deduce specific contact resistance of about 1.1 mΩ·cm^2 for ITO/Ti. Given that emitter fractions in the range of 49-71 % are defined in the solar cells (see table 2), this value is low enough to introduce a negligible impact on *FF*. Consequently, Ti is used as metal contact in the final devices.

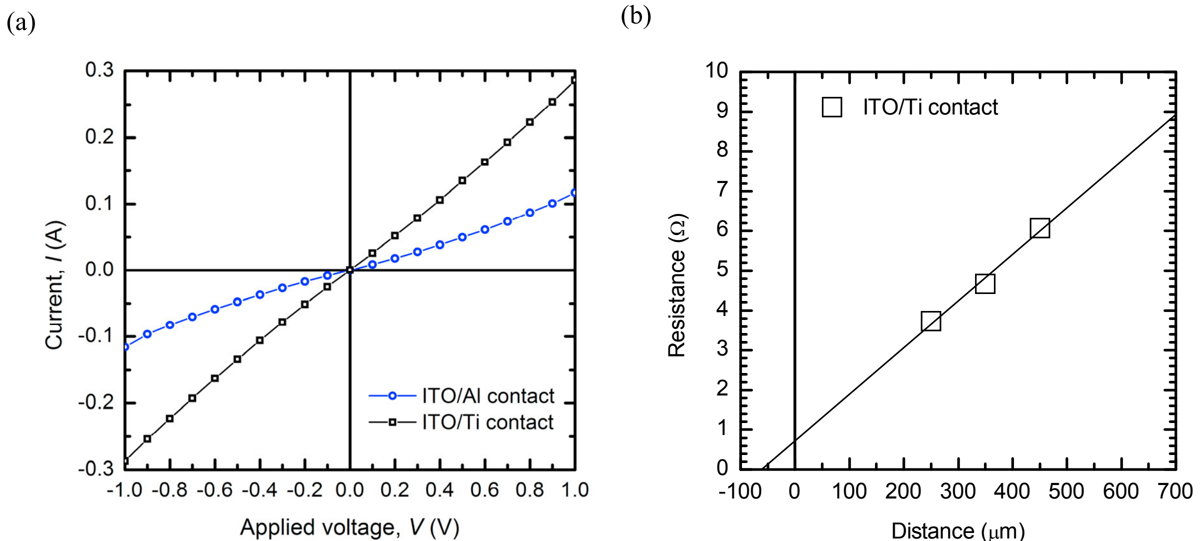

Fig. 3. (a) Measured current of ITO/Al contact and ITO/Ti contact (b) Total resistance as a function of contact spacing;

3.3 Solar cell results

Following the fabrication process explained above, we finished six 3x3 cm^2 solar cells in two 4" wafers. The photovoltaic parameters as a function of the emitter contact fraction (f_e) are shown in table 2. As it can be seen, except for one cell, the rest have a conversion efficiency in the 18-19 % range with a champion cell of 19.0 % with V_{oc} = 677 mV, J_{sc} = 40.7 mA/cm^2 and FF = 68.8 %. Focusing on J_{sc}, the obtained values are higher than the ones reported in reference [1] for fully laser-processed cells. The measured External Quantum Efficiency (*EQE*) curve of the champion cell is shown in Figure 4.(a) together with the one reported in reference [1] for a direct comparison. The increase in J_{sc} corresponds to higher *EQE* values for $\lambda < 1000$ nm. This constant increase is attributed to a better front surface passivation. On the other hand, V_{oc} values have significantly increased from the 620-644 mV reported in reference [1] to 665-684 mV, demonstrating a lower recombination in the SHJ emitter compared to the laser-doped one. Finally, despite *FF* values are better than the ones related to fully laser doped cells (57-65 %), this parameter is clearly limiting cell efficiency.

Table 2. Photovoltaic figures of 3x3 cm^2 p-type hybrid cells with ITO of ~80 Ω/square.

f_e (%)	J_{sc} (mA/cm^2)	V_{oc} (mV)	*FF(pFF)* (%)	η (%)
71%(wafer1)	39.6	666	58.3(77.1)	15.4
71%(wafer2)	41.2	674	65.0(77.2)	18.0
60%(wafer1)	39.8	665	71.0(82.1)	18.8
60%(wafer2)	40.7	677	68.8(81.0)	19.0
49%(wafer1)	40.5	684	65.7(81.8)	18.2
49%(wafer2)	40.9	671	69.1(80.7)	19.0

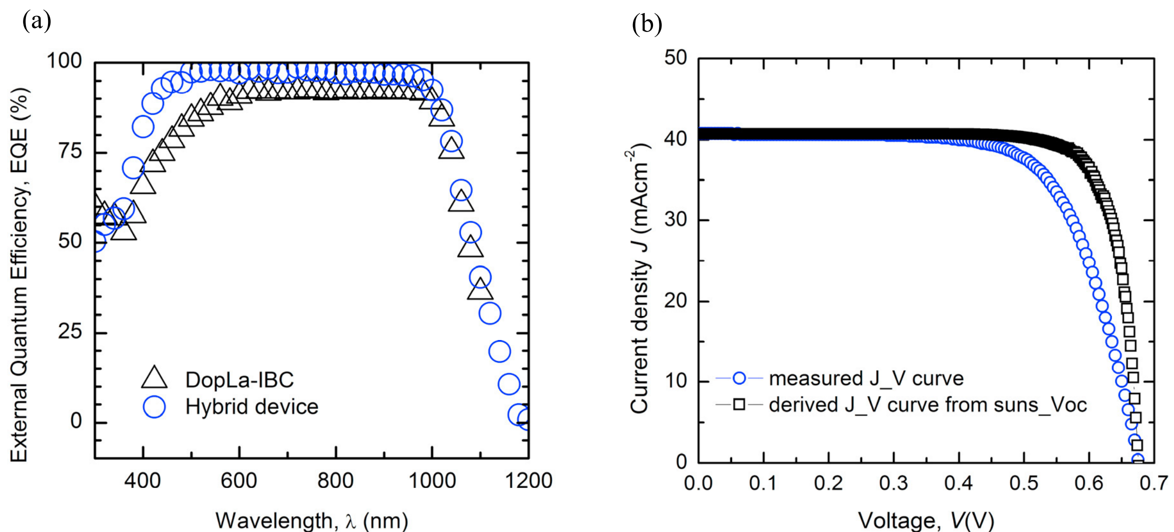

Fig. 4. (a) EQE measurements of fabricated devices. (b) J-V curve (cell1) of the solar cell with best efficiency

In order to get a deeper insight of the origin of the low *FF*, we measured *Suns-*V_{oc} curves and calculated the corresponding *pseudo-FF* (*pFF*), where ohmic losses have no impact [14]. Apart from cells with f_e= 71 % that show *pFF* of about 77 % limiting the FF to even lower values, the rest of the cells have a *pFF* well beyond 80 % indicating a good junction formation with low shunting. Thus, a transport problem must be behind the low *FF* values. A possible candidate is the distance between base contacts. However, *FF* as high as 74 % have been reported in reference [15] where we applied identical geometry to the base contacts. Thus, the origin of the low *FF* in these hybrid solar cells should be related to the amorphous silicon emitter.

In the previous section, we determined a low contact resistance of ITO/Ti contact that in any case could significantly contribute to the series resistance of the device. Therefore, in our opinion the most probable origin of the low *FF* is the low conductivity of the phosphorus-doped a-Si:H film. Our group developed this film contacted by ITO to be located at the front surface where the light impinges the cell [12],[16]. There, the conductivity of amorphous silicon layer is enhanced due to photogenerated carriers allowing an efficient transport of majority carriers. However, in the case of back contact heterojunction, photogeneration is negligible and the low conductivity cannot be compensated. Moreover, a small reduction in the slope in *J-V* curves close to V_{oc} is also observed in some of our hybrid cells resembling an "S" shape. This type of *J-V* curve distortion is reported for low doped a-Si:H layers in rear emitter configuration cells [17]. Consequently, future works will address this problem in order to fully exploit the potential of our hybrid devices.

4. Conclusions

In this work, we have reported on hybrid p-type solar cells where the emitter is based on SHJ technology while the base contacts are created by laser processing Al_2O_3/SiC_x films. The combination of these two kind of junction formation is proved to effectively enhance the solar cell conversion efficiency compared to a fully laser-processed solar cells, especially the V_{oc} value which benefits from the lower recombination in SHJ emitter compared to the laser doped one. We have also demonstrated the compatibility of both involved technologies while keeping the fabrication process at low temperature (< 400 ºC). In particular, a strong impact on Al_2O_3/c-Si interface is observed after the CF_4/O_2 plasma used to etch the capping SiC_x layer. Surface passivation is recovered after replacing the Al_2O_3 film by the a-Si:H(i/n)+ITO stack. On the other hand, Titanium is used for simultaneously contacting ITO and laser spots with specific contact resistance of ITO/Ti of 1.1 $m\Omega\cdot cm^2$. Finally, efficiencies as high as 19.0 % are reported for these hybrid devices, in which the low conductivity of the phosphorus-doped a-Si:H layer is considered as the main limiting factor.

Acknowledgements

This work have been supported by MINECO through projects ENE2013-48629-C4-1-R and TEC2014-59736-R. C. Jin thanks the China Scholarship Council (CSC) for the financial support.

References

[1] López G, Ortega PR, Martín I, Voz C, Orpella A, Alcubilla R. "Cold" Process for IBC c-Si Solar Cells Fabrication. Energy Procedia 2016; 92: 652–660.
[2] Martín I, Colina M, Coll A, López G, Ortega P, Orpella A, Alcubilla R. c-Si Solar Cells based on Laser-processed Dielectric Films. Energy Procedia 2014; 55: 255–264.
[3] Martín I, Ortega P, Colina M, Orpella A, López G, Alcubilla R. Laser processing of Al 2 O 3 /a-SiC x :H stacks: a feasible solution for the rear surface of high-efficiency p-type c-Si solar cells: Laser processing of Al 2 O 3 /a-SiC x :H stacks. Progress in Photovoltaics: Research and Applications 2013: 21, 5; 1171-1175.
[4] Ortega P, Martín I, Lopez G, Colina M, Orpella A, Voz C, Alcubilla R. p-type c-Si solar cells based on rear side laser processing of Al2O3/SiCx stacks. Solar Energy Materials and Solar Cells 2012; 106: 80–83.
[5] Yoshikawa K, Kawasaki H, Yoshida W, Irie T, Konishi K, Nakano K, Uto T, Adachi D, Kanematsu M, Uzu H, Yamamoto K. Silicon heterojunction solar cell with interdigitated back contacts for a photoconversion efficiency over 26%. Nature Energy 2017; 2: 17032.
[6] Masuko K, Shigematsu M, Hashiguchi T, Fujishima D, Kai M, Yoshimura N, Yamaguchi T, Ichihashi Y, Mishima T, Matsubara N, Yamanishi T, Takahama T, Taguchi M, Maruyama E, Okamoto S. Achievement of More Than 25% Conversion Efficiency With Crystalline Silicon Heterojunction Solar Cell. IEEE Journal of Photovoltaics 2014; 4: 1433–1435.
[7] Descoeudres A, Holman ZC, Barraud L, Morel S, De Wolf S, Ballif C. > 21% efficient silicon heterojunction solar cells on n-and p-type wafers compared. IEEE Journal of Photovoltaics 2013; 3: 83–89.
[8] Richter A, Glunz SW, Werner F, Schmidt J, Cuevas A. Improved quantitative description of Auger recombination in crystalline silicon. Physical Review B 2012; 86: 165202.
[9] Hoex B, Gielis JJH, van de Sanden MCM, Kessels WMM. On the c-Si surface passivation mechanism by the negative-charge-dielectric Al2O3. Journal of Applied Physics 2008; 104: 113703.

[10] Nicollian EH, Brewster JR. MOS (Metal Oxide Semiconductor) Physics and Technology, New Jersey: John Wiley & Sons, Inc; 2003, p.319-331
[11] Terman LM. An investigation of surface states at a silicon/silicon oxide interface employing metal-oxide-silicon diodes 1962; 5: 285-299.
[12] Morales-Vilches AB, Voz C, Colina M, Munoz-Martin D, Martin I, Ortega PR, Lopez-Rodriguez G, Molpeceres C, Alcubilla R. Study of the Surface Recombination Velocity for Ultraviolet and Visible Laser-Fired Contacts Applied to Silicon Heterojunction Solar Cells. IEEE Journal of Photovoltaics 2015: 5, 1006–1013.
[13] Schroder DK. Semiconductor Material and Device Characterization 3rd Edition. New York: Wiley-IEEE Press; 2015.
[14] Sinton RA, Cuevas A. A quasi-steady-state open-circuit voltage method for solar cell characterization, in: Proceedings of the 16th European Photovoltaic Solar Energy Conference 2000; pp. 1152-1155.
[15] Masmitja G, Gerling LG, Ortega P, Puigdollers J, Martín I, Voz C, Alcubilla R. V_2O_x-based hole-selective contacts for c-Si interdigitated back-contacted solar cell. submitt to Journal of Materials Chemistry A.
[16] Colina M, Morales-Vilches A, Voz C, Martín I, Ortega P, Orpella A, López G, Alcubilla R. Laser Induced Forward Transfer for front contact improvement in silicon heterojunction solar cells. Applied Surface Science 2015; 336, 89–95.
[17] Desrues T, Ribeyron PJ, Vandeneynde A, Ozanne AS, Souche F, Muñoz D, Denis C, Diouf D, Kleider JP, B-doped a-Si:H contact improvement on silicon heterojunction solar cells and interdigitated back contact structure. Phys. Status Solidi (c) 2010; 7: 1011–1015.